MODELLING AND EVALUATING CARBAMATE POLYMERIZATION OF MONOETHANOLAMINE IN POST-COMBUSTION CARBON CAPTURE

Lucas Braakhuis[1], Hanna K. Knuutila[1*]

[1] Department of Chemical Engineering, Norwegian University of Science and Technology, 7491 Trondheim, Norway

* Corresponding author e-mail: hanna.knuutila@ntnu.no

Abstract

In this work, experimental data on carbamate polymerization of aqueous solutions of monoethanolamine (MEA) has been collected and analyzed. Three degradation models were developed describing thermal degradation of MEA in aqueous solutions to investigate the importance of taking into account MEA consumption when describing the experimental data. The models were fitted to literature data. It was found that with the same number of parameters, a better fit was obtained when considering MEA consumption. All the models showed increased deviations for longer experiments and at higher temperatures, indicating that the high concentration of degradation compounds might influence the degradation rate.

Keywords: *MEA, monoethanolamine, carbamate polymerization, thermal degradation, solvent management.*

1. Introduction

One of the most promising ways to reduce carbon dioxide emissions into the atmosphere is through absorption-based post-combustion carbon capture. In this process, exhaust gases from industry are treated with a water-based solvent, which selectively absorbs the CO_2 from the gas. The solvent is stripped at elevated temperatures, after which it is recycled. A fraction of the solvent is entrained in the flue gas or lost through degradation and is replaced. One of the main challenges is to reduce the loss of solvent through degradation and prevent the formation of degradation products [1].

Solvents degrade when brought into contact with oxygen in the absorber or through carbamate polymerization at increased temperatures and under the presence of CO_2. Carbamate polymerization, typically happening during solvent regeneration in the stripper, is also referred to as thermal degradation under the presence of CO_2. Aqueous 30 wt-% of monoethanolamine (MEA) solution is one of the most established solvents used for post-combustion carbon capture [2] and the solvent studied in this paper.

Figure 1 gives an overview of the predominant degradation reactions and products. The carbamate that is formed when CO_2 reacts with MEA can undergo a ring closure to form 2-oxazolidone (OZD). Concentrations of this compound are low in degraded solutions, and therefore, OZD is suspected to be an intermediate [3]. OZD can react with free MEA to form N-(2-hydroxyethyl)-ethylenediamine (HEEDA), which in turn can react with CO2 to form 1-(2-hydroxyethyl)-2-imidazolidone (HEIA).

Léonard et al. [4] modelled the carbamate polymerization rate as the product of a temperature-dependent reaction rate coefficient and the initial concentration of CO_2. Because of the abundance of MEA, it was assumed the amine concentration did not affect the degradation rate. However, experimental data shows that the degradation rate is not constant and tends to decrease over time, especially at higher temperatures and loadings [5]. This indicates that the consumption of MEA might play an important role when modeling laboratory-scale degradation data.

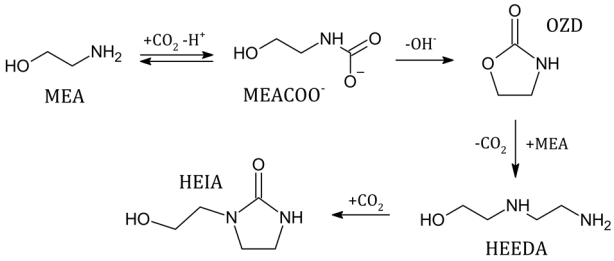

Figure 1**:** Overview of the most significant carbamate polymerization reactions, as proposed by [3], [5]–[7].

In this study, three different degradation models were developed, fitted, and evaluated to investigate the extent and effect of this consumption.

2. Methodology

Experimental data from carbamate polymerization studies given in Table 1 was used in this work. No additional degradation experiments were performed. The experimental methods in these studies were similar to each other. Amine solutions were prepared and loaded with CO_2 up to the specified loading. The solution was transferred into stainless steel cylinders, which were closed off. The cylinders' liquid volume and headspace varied slightly in the different experiments but were in the same order of magnitude. Next, the cylinders were placed in a heat-controlled chamber and kept at a specified temperature for a duration of time. During this time, no stirring or agitation took place. After the degradation, the cylinders were removed and cooled down. The solutions were then analyzed using different analytical methods. The MEA concentration was typically analyzed with (HP)LC-MS and/or Ion

Chromatography (IC). In some cases, analysis via GC-MS or LC-MS was used to identify and quantify degradation products. The uncertainty in these analytical methods is assumed to be the same, so each datapoint can be weighted equally.

Table 1: Overview of the experimental data on carbamate polymerization used in this study.

Datapoints	Loading, α	Temperature	Reference
30	0.2 - 0.5	100 - 150	[5]
9	0.1 - 0.4	105 - 135	[8]
25	0.1 - 0.5	135	[3]
5	0.5	135	[9]
6	0.44	120 - 140	[4]
8	0.4	135	[10]
3	0.4	125 - 145	[11]
2	0.4	135	[12]

2.1 Proposed degradation models

The model equations are given in Table 2. The first model describes linear degradation, similar to the model by Léonard et al. [4]. The initial concentration ($[MEA]_0$) has been taken into account to account for different starting concentrations of MEA. The second model takes into account the consumption of MEA, while the CO_2 concentration is kept constant at its initial concentration.

The approach behind the third model is slightly different. Considering the degradation mechanism in Figure 1, one would expect the degradation rate of MEA to be proportional to the concentration of MEA-carbamate. Therefore, this model aims to predict the carbamate concentration, which is then used to fit the reaction rate. Since no experimental data is available on the speciation at these temperatures, the carbamate concentration is modeled with an in-house vapor-liquid equilibrium model calculating activities using an eNRTL-model.

Table 2: Short description and equations of the investigated degradation models in this work.

	Description	Equations
M1	Linear degradation	$\frac{d[\mathrm{MEA}]}{dt} = k(T) \cdot [\mathrm{MEA}]_0[\mathrm{CO_2}]_0$
M2	MEA consumption	$\frac{d[\mathrm{MEA}]}{dt} = \mathrm{k}(T) \cdot [\mathrm{MEA}][\mathrm{CO_2}]_0$
M3	MEA consumption, CO2SIM speciation	$\frac{d[\mathrm{MEA}]}{dt} = \mathrm{k}(T) \cdot [\mathrm{MEACOO^-}]$ $[\mathrm{MEACOO^-}] = f([\mathrm{MEA}], [\mathrm{CO_2}]_0)$

2.1 Adjusted form of the Arrhenius equation

For all models, the reaction rate coefficient at a specified temperature ($k(T)$) is determined using an adjusted form of the Arrhenius equation (1). Here T_r and k_r are the reference temperature and the reaction rate coefficient at reference temperature, respectively. A reference temperature of 400 K has been chosen as this is the rough average of the experiments. This adjusted form yields the same results, but provides a more meaningfull expression for the reaction rate coefficient, which allows for better model comparison and more intuitive initial estimates.

$$\mathrm{k}(T) = k_\mathrm{r} \cdot \exp\left(\frac{-E_A}{R}\left(\frac{1}{T} \quad \frac{1}{T_\mathrm{r}}\right)\right) \tag{1}$$

2.2 Fitting the parameters

The model parameters have been fitted by minimizing the relative least square errors between the experimental data and the model results. Each experiment is treated individually and weighted equally. Optimization has been performed using the nonlinear Levenberg-Marquardt algorithm. In addition, a particle swarm optimization (PSO) algorithm was used to check if the solution was a valid global minimum. Both routines yielded the same optimized parameters for all the investigated cases.

2.3 Complete and refined dataset

There appears to be no explicit agreement between the experimental results at higher temperatures and loadings (above 145 °C or α = 0.5). The relative deviation between the data sets is significantly larger than for experiments at more moderate temperatures and lower loadings. The reason for this difference is not known, but it may be caused by experimental challenges at high temperatures and loadings. Because only four experiments were performed at these extreme conditions, without clear agreement between them, the three models shown in Table 2 have been evaluated with both the complete dataset, taking into account all the data in Table 1 and by excluding experimental data above 145 °C or at a loading of 0.5 (refined dataset).

2.4 Pure experimental error

There were eight sets of replicate degradation experiments in the dataset (17 datapoints in total), for which the temperature, loading, initial concentration, and degradation time were the same (seven sets at 135 °C with various loadings, one at 120 °C with a loading of 0.4). These replicates were used to get an indication of the sum of pure experimental errors (SSEP). The sum of squared erros (SSE) of the model in relation to the expirmental data is made up out of the SSEP and the sum of square erros caused by limitations in the model, the lack of fit (SSELOF). The part of the SSE, which the pure error cannot explain is thus caused by lack of fit.

The degree of the lack of fit of the model can be evaluated by comparing the mean error due to lack of fit (MSELOF) against the mean pure square error (MSEP). This fraction is then compared to a F-distribution at 95%-confidence, which is dependent on the total number of datapoints and the number of replicates, see equation (2). The model is considered to be inadequate if $T_\mathrm{LOF} \geq 1$.

$$T_\mathrm{LOF} = \frac{\frac{\mathrm{MSELOF}}{\mathrm{MSEP}}}{F_{0.95,\nu_\mathrm{LOF},\nu_\mathrm{pure}}} \tag{2}$$

3. Results

Table 3: Fitted model parameters, confidence intervals and lack-of-fit tests for the complete dataset. Data used to fit the models covers temperature and loading range of 100 – 150 °C and α: 0.1 – 0.5.

Model	Rate parameters	Units	Confidence intervals (95%)	T_{LOF}
M1	$k_r = 6.05 \cdot 10^{-11}$ $E_A = 3.16 \cdot 10^4$	$[m^3 \cdot mol^{-1} \cdot s^{-1}]$ $[J \cdot mol^{-1}]$	$[4.97\text{-}7.12] \cdot 10^{-11}$ $[1.95\text{-}4.38] \cdot 10^4$	6.201
M2	$k_r = 7.02 \cdot 10^{-11}$ $E_A = 8.87 \cdot 10^4$	$[m^3 \cdot mol^{-1} \cdot s^{-1}]$ $[J \cdot mol^{-1}]$	$[5.68\text{-}8.36] \cdot 10^{-11}$ $[0.68\text{-}1.08] \cdot 10^5$	2.757
M3	$k_r = 3.91 \cdot 10^{-7}$ $E_A = 1.22 \cdot 10^5$	$[s^{-1}]$ $[J \cdot mol^{-1}]$	$[2.81\text{-}5.01] \cdot 10^{-7}$ $[0.90\text{-}1.54] \cdot 10^5$	3.671

Table 4: Fitted model parameters, confidence intervals and lack-of-fit tests for the refined dataset. Data used to fit the models covers temperature and loading range of 100 – 145 °C and α: 0.1 – 0.45.

Model	Rate parameters	Units	Confidence intervals (95%)	T_{LOF}
M1	$k_r = 2.71 \cdot 10^{-11}$ $E_A = 1.38 \cdot 10^5$	$[m^3 \cdot mol^{-1} \cdot s^{-1}]$ $[J \cdot mol^{-1}]$	$[2.16\text{-}3.25] \cdot 10^{-11}$ $[1.06\text{-}1.69] \cdot 10^5$	0.309
M2	$k_r = 3.34 \cdot 10^{-11}$ $E_A = 1.39 \cdot 10^5$	$[m^3 \cdot mol^{-1} \cdot s^{-1}]$ $[J \cdot mol^{-1}]$	$[2.88\text{-}4.01] \cdot 10^{-11}$ $[1.14\text{-}1.64] \cdot 10^5$	0.175
M3	$k_r = 1.76 \cdot 10^{-7}$ $E_A = 1.58 \cdot 10^5$	$[s^{-1}]$ $[J \cdot mol^{-1}]$	$[1.42\text{-}2.10] \cdot 10^{-7}$ $[1.29\text{-}1.87] \cdot 10^5$	0.187

Table 3 shows that the lack-of-fit test parameter is larger than 1 for each model. This shows that the residuals of the models are significantly larger than can be explained by the pure experimental error and thus, the full dataset cannot be fitted appropriately. The contribution of experiments at higher temperatures and loadings to the SSE was significant, however, a clear trend was not observed. There were no replicates for the experiments at higher temperatures and loadings, so the pure experimental error was the same for both datasets.

Excluding the data at high temperatures (145 °C and above) improves the models ability to represent the experimental data significantly, as seen in

Table 4. When comparing these to the results in Table 3, the fitted activation energy is higher and the reaction rates lower for the total dataset, resulting in a higher temperature dependency of the reaction rate. It would be good to investigate how reproducible the degradation experiments at temperatures above 145 °C or with a loading of 0.5 are, to evaluate their experimental error. For now, we will focus on the results from the refined dataset.

Table 4 shows also that model 2 and 3 have a much better fit than the linear model (model 1). Because model 2 considers the consumption of MEA, the reaction rate coefficient is expected to be slightly larger than for model 1, as the concentration of MEA will decrease over time. The reaction rate coefficient for model three is several orders of magnitude higher because in this model, the reaction rate coefficient is only multiplied with the concentration of MEA-carbamate, instead of both the concentration of CO_2 and MEA, which is the case for the other models. In addition, the activation energy is higher for this model. Overall, model 2 has the best fit, but there is no significant difference between model 2 and 3.

In Figure 2, several of the datapoints are compared to the fitted results of model 2. The experimental data by Davis et al. shows less degradation in comparison to the other experiments. Overall the model fits the experimental data adequately, with a relative standard deviation of 5.02% (6.29% and 5.15% for model 1 and 3 respectively).

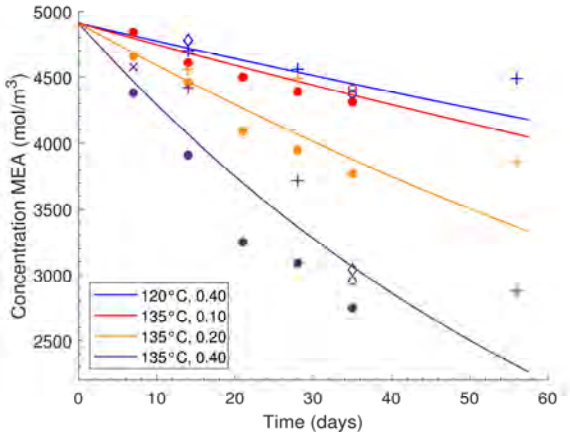

Figure 2: Model 2 results compared with experimental data. Markers indicate experiments from Grimstvedt (o), Davis (+), Fytianos (◊), Eide-Haugmo (•), and Huang (x).

3.1 Compared model predictions

The degradation experiments can replicate operational conditions but are not necessarily comparable. The cylinders in the degradation experiments are closed off, so consumption of the solvent and CO_2 will influence concentrations and degradation rates. In a continuous capture plant there will be a constant supply of CO_2 from the flue gas and a make-up of degraded solvent, so the conditions in for example the reboiler will not change significantly.

Measurements at lower solvent concentrations are thus not representable, however, they can still be used, as they provide useful insight into the degradation mechanism. To evaluate and compare the predicted

degradation rates at continuous operation, the initial degradation rate is more interesting, because the initial conditions and concentrations of MEA and CO_2 are more representative of the actual process. The predicted degradation rates are given in Figure 3.

In comparison, the degradation models show similar trends with temperature at different loadings. Model 2, which had the best fit, predicts the most degradation. In comparison, the linear degradation model (model 1) predicts less degradation, especially at higher temperatures. This is because at higher temperatures, the concentration of MEA is reduced significantly and the degradation rate is also reduced over time.

As a result, the linear concentration slope of MEA is less steep and less degradation is predicted. The higher activation energy in model 3 also becomes apparent as the degradation rate increases more rapidly with temperature. The model by Léonard et al. ([4]) is conservative with respect to the models fitted in this study. With a loading of 0.4 and at a stripper temperature of 120 °C, the degradation rate predicted by model 2 is 47.5% higher than the degradation as predicted by the model of Léonard et al.. At the same conditions, model 2 also predicts 25.9% more degradation than model 1.

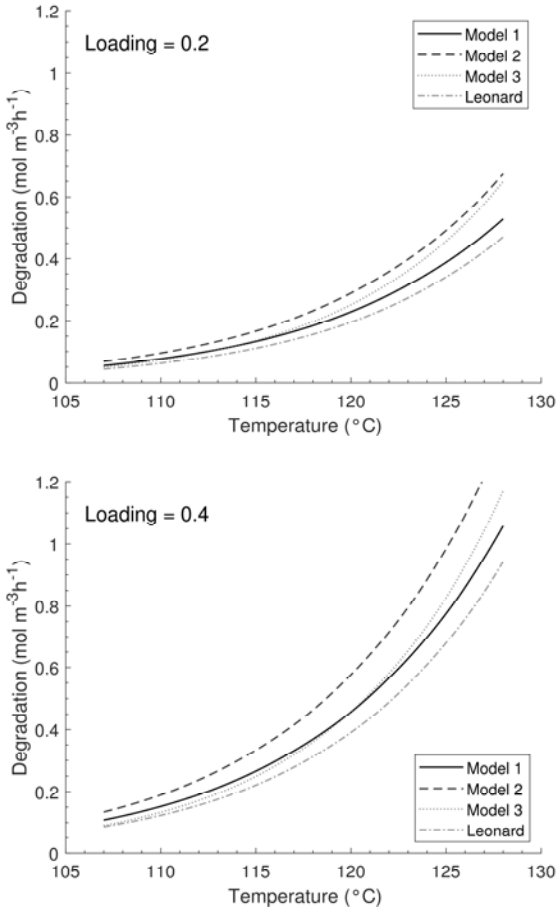

Figure 3: Predicted degradation rate due to carbamate polymerization for 30 wt-% MEA at a loading of 0.2 (above) and 0.4 (below). The kinetic model by Léonard et al. ([4]) is evaluated as a reference.

3.2 Joint confidence region

The marginal confidence intervals of the fitted parameters are relatively large. The correlation between the activation energy and the reaction rate coefficient at reference temperature was also significant for all models, but lowest for model 2 at 0.956. For this model, the approximate confidence region of 95% was determined and is given in Figure 4. From this figure, the strong correlation between the parameters is also apparent.

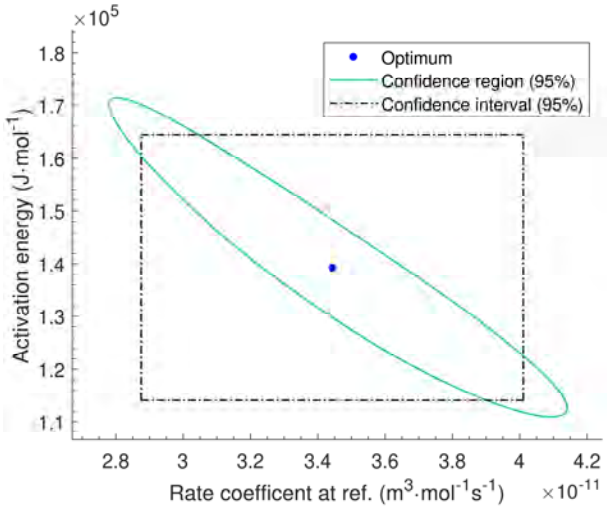

Figure 4: Marginal confidence interval and joint confidence region for the parameter estimates of model 2 on the refined dataset.

3.3 Residual plots

The residuals for model 2 are analysed in Figure 5. The errors appear to be randomly distributed as a function of the loading since no clear pattern can be observed. The temperature, on the other hand, is strongly correlated with the error. This also explains why the regression was more accurate for the refined dataset. There also appears to be a slight increase in the residuals when the experiments last longer. The effect, however, is more pronounced than in the case of temperature.

These trends indicate that the error is most likely not purely analytical and that fluctuations in experimental conditions play a role as well. These fluctuations could cause the reaction rate to deviate, resulting in larger errors in solvent concentration over time. It's thus recommended to investigate the cause and extent of these fluctuations.

Model 1 was found to underpredict the degradation at first, while overpredicting experiments with a longer duration. This shows that the model was unable to represent the non-linear degradation data, and explains the higher lack-of-fit parameter for the model.

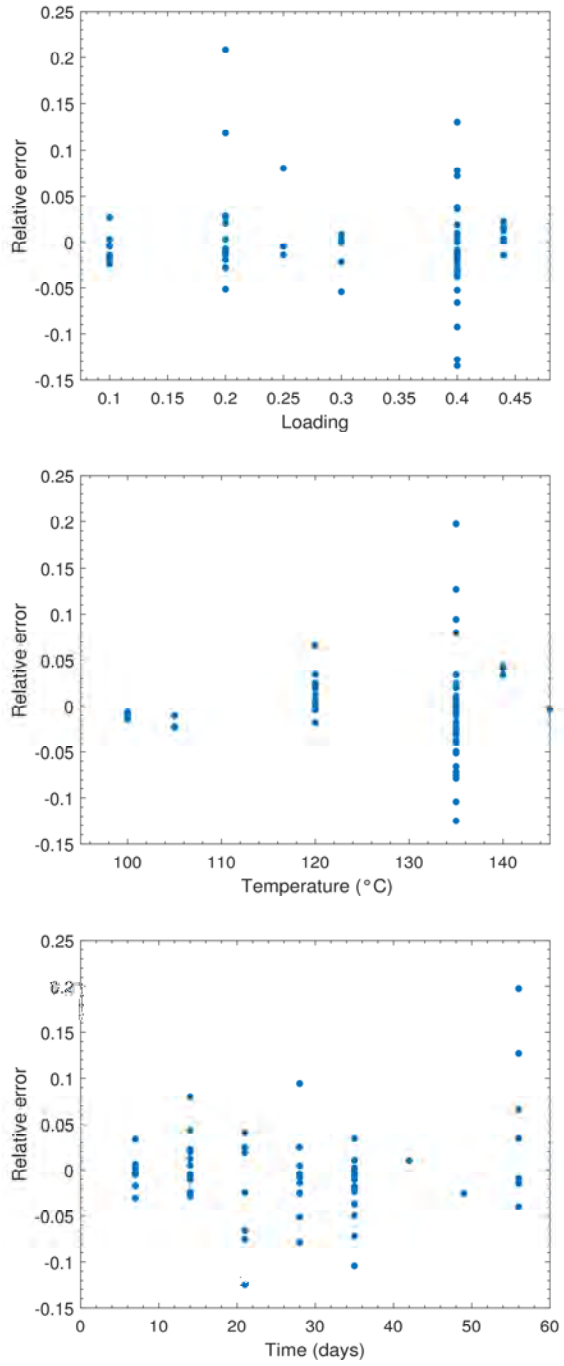

Figure 5: Relative error as a function of initial loading (top), temperature (middle), and experiment duration (bottom) for the parameter estimates of model 2 on the refined dataset.

4. Conclusion

To conclude, three models have successfully been used to evaluate and predict degradation through carbamate polymerization. Model 2, which takes into account the consumption of MEA in the rate equation, was able to explain the experimental data most accurately, with a relative standard deviation of 5.02%, compared to 6.29% and 5.15% for model 1 and 3 respectively. Model 2 predicts over 25.9% more carbamate polymerization at stripper conditions compared to model 1, the linear model, which do not take into account the concentration of MEA over time.

The use of the speciation model to determine the carbamate concentration, in Model 3, also showed promise. It would be interesting to investigate how this model behaves when the concentration of CO_2 and some of the major degradation products were also taken into account. Another recommendation is to perform more degradation experiments at increased temperatures and loadings to evaluate the experimental uncertainty.

Acknowledgements

This publication has been produced with support from the NCCS Centre, performed under the Norwegian research program Centres for Environment-friendly Energy Research (FME). The authors acknowledge the following partners for their contributions: Aker Solutions, ANSALDO Energia, CoorsTek Membrane Sciences, EMGS, Equinor, Gassco, KROHNE, Larvik Shipping, Norcem, Norwegian Oil and Gas, Quad Geometrics, Shell, TOTAL, and the Research Council of Norway (257579/E20).

References

[1] F. Vega, A. Sanna, B. Navarrete, M. M. Maroto-Valer, and V. J. Cortés, 'Degradation of amine-based solvents in CO2 capture process by chemical absorption', *Greenh. Gases Sci. Technol.*, vol. 4, no. 6, pp. 707–733, 2014, doi: https://doi.org/10.1002/ghg.1446.

[2] C. Gouedard, D. Picq, F. Launay, and P.-L. Carrette, 'Amine degradation in CO2 capture. I. A review', *Int. J. Greenh. Gas Control*, vol. 10, pp. 244–270, Sep. 2012, doi: 10.1016/j.ijggc.2012.06.015.

[3] I. Eide-Haugmo, 'Environmental impacts and aspects of absorbents used for CO2 capture.', Norwegian University of Science and Technology, Trondheim, 2011.

[4] G. Léonard, D. Toye, and G. Heyen, 'Experimental study and kinetic model of monoethanolamine oxidative and thermal degradation for post-combustion CO 2 capture', *Int. J. Greenh. Gas Control*, vol. 30, pp. 171–178, Nov. 2014, doi: 10.1016/j.ijggc.2014.09.014.

[5] J. Davis and G. Rochelle, 'Thermal degradation of monoethanolamine at stripper conditions', *Energy Procedia*, vol. 1, no. 1, Art. no. 1, Feb. 2009, doi: 10.1016/j.egypro.2009.01.045.

[6] H. Lepaumier, D. Picq, and P.-L. Carrette, 'New Amines for CO 2 Capture. I. Mechanisms of Amine Degradation

in the Presence of CO 2', ***Ind. Eng. Chem. Res.***, vol. 48, no. 20, Art. no. 20, Oct. 2009, doi: 10.1021/ie900472x.

[7] E. F. da Silva ***et al.***, 'Understanding 2-Ethanolamine Degradation in Postcombustion CO 2 Capture', ***Ind. Eng. Chem. Res.***, vol. 51, no. 41, Art. no. 41, Oct. 2012, doi: 10.1021/ie300718a.

[8] A. Grimstvedt, E. Falck da Silva, and K. A. Hoff, 'Thermal degradation of MEA, effect of temperature and CO2 loading', SINTEF Materials and Chemistry, Trondheim, TCCS-7, 2013.

[9] H. Lepaumier ***et al.***, 'Comparison of MEA degradation in pilot-scale with lab-scale experiments', ***Energy Procedia***, vol. 4, pp. 1652–1659, Jan. 2011, doi: 10.1016/j.egypro.2011.02.037.

[10] S. Zhou, S. Wang, and C. Chen, 'Thermal Degradation of Monoethanolamine in CO 2 Capture with Acidic Impurities in Flue Gas', ***Ind. Eng. Chem. Res.***, vol. 51, no. 6, Art. no. 6, Feb. 2012, doi: 10.1021/ie202214y.

[11] Q. Huang ***et al.***, 'Impact of Flue Gas Contaminants on Monoethanolamine Thermal Degradation', ***Ind. Eng. Chem. Res.***, vol. 53, no. 2, pp. 553–563, Jan. 2014, doi: 10.1021/ie403426c.

[12] G. Fytianos, S. Ucar, A. Grimstvedt, A. Hyldbakk, H. F. Svendsen, and H. K. Knuutila, 'Corrosion and degradation in MEA based post-combustion CO2 capture', ***Int. J. Greenh. Gas Control***, vol. 46, pp. 48–56, Mar. 2016, doi: 10.1016/j.ijggc.2015.12.028.